Cell

Cyclic Dinucleotides Trigger ULK1 (ATG1) Phosphorylation of STING to Prevent Sustained Innate Immune Signaling

Hiroyasu Konno,[1] Keiko Konno,[1] and Glen N. Barber[1,*]
[1]Department of Cell Biology and Sylvester Comprehensive Cancer Center, University of Miami School of Medicine, Miami, FL 33136, USA
*Correspondence: gbarber@med.miami.edu
http://dx.doi.org/10.1016/j.cell.2013.09.049

SUMMARY

Activation of the stimulator of interferon genes (STING) pathway by microbial or self-DNA, as well as cyclic dinucleotides (CDNs), results in the induction of numerous genes that suppress pathogen replication and facilitate adaptive immunity. However, sustained gene transcription is rigidly prevented to avoid lethal STING-dependent proinflammatory disease by mechanisms that remain unknown. We demonstrate here that, after autophagy-dependent STING delivery of TANK-binding kinase 1 (TBK1) to endosomal/lysosomal compartments and activation of transcription factors interferon regulatory factor 3 (IRF3) and NF-κB, STING is subsequently phosphorylated by serine/threonine UNC-51-like kinase (ULK1/ATG1), and IRF3 function is suppressed. ULK1 activation occurred following disassociation from its repressor AMP activated protein kinase (AMPK) and was elicited by CDNs generated by the cGAMP synthase, cGAS. Thus, although CDNs may initially facilitate STING function, they subsequently trigger negative-feedback control of STING activity, thus preventing the persistent transcription of innate immune genes.

INTRODUCTION

Host cells have evolved a variety of mechanisms to recognize and eliminate invading microbes, including developing the ability to recognize pathogen-associated proteins and nucleic acid and subsequently invoke powerful cellular signaling events that stimulate the production of innate immune genes (Blasius and Beutler, 2010; Kawai and Akira, 2011; Tamura et al., 2008). Such defenses include the Toll-like receptors (TLR), the RIG-I (RLR) family of receptors and nucleotide-binding domain, and leucine-rich repeat-containing (NLR) receptors that sense microbial molecules such as CpG DNA, viral RNAs, and lipopolysaccharides (Blasius and Beutler, 2010; Kawai and Akira, 2011; Tamura et al., 2008). In addition, an endoplasmic reticulum (ER)-associated molecule referred to as stimulator of interferon genes (STING) has recently been shown to control a new sensing pathway that is essential for detecting aberrant cytosolic DNA species and for triggering the production of host defense genes such as type I interferon (IFN) (Ishikawa and Barber, 2008; Ishikawa et al., 2009).

The activation of STING (also referred to as TMEM 173/MPYS/MITA/ERIS) may involve direct association with cytosolic DNA species as well as with cyclic dinucleotides (cyclic diguanosine monophosphate [GMP] or AMP) generated directly from certain intracellular bacteria or via a DNA-binding protein cGAS (cGAMP synthase, also known as male abnormal 21 domain containing 1 [Mab-21 domain containing1/MB21D1] or C6orf150) (Burdette et al., 2011; Diner et al., 2013; Jin et al., 2008; Sun et al., 2009, 2013; Woodward et al., 2010; Zhong et al., 2008). However, following the detection of cytosolic DNA, cGAS utilizes GTP and ATP to generate noncanonical 2′ to 5′ cyclic GMP-AMP (cGAMP) rather than 3′ to 5′ canonical cyclic dinucleotide species generally generated by bacteria (Ablasser et al., 2013; Civril et al., 2013; Gao et al., 2013; Kranzusch et al., 2013; Zhang et al., 2013). Activated STING, accompanied by TANK-binding kinase 1 (TBK1), then undergoes dramatic autophagy-related trafficking involving ATG9 and associates with endosomes containing the transcription factors interferon regulatory factor 3 (IRF3) and NF-κB (Ishikawa et al., 2009; Saitoh et al., 2009). Phosphorylated IRF3 and activated NF-κB translocate to the nucleus to initiate the transcription of numerous innate immune genes, including IFN and members of the IFIT family (Abe et al., 2013).

However, although STING has been shown to be essential for the protection of the host against DNA pathogens, sustained STING stimulation, such as by self-DNA, has also been shown to be responsible for lethal inflammatory disease in at least two murine models (*DnaseII*$^{-/-}$ and *DnaseIII*/*Trex1*$^{-/-}$) and plausibly may therefore play a key role in inflammatory/autoimmune disease in humans (Ahn et al., 2012; Gall et al., 2012). Thus, although STING is essential for initiating host defense counter measures, chronic STING activity needs to be controlled to avoid the deleterious consequences that sustained innate immune gene induction would have upon the host. Here, we demonstrate that, after activation and trafficking, STING is phosphorylated by UNC-51-like kinase (ULK1). This occurs following ULK1 dissociation from its repressor AMPK and was found to be triggered by cGAS-generated CDNs. Therefore, although CDNs may initially facilitate STING activity, they also initiate a negative-feedback control mechanism to thwart

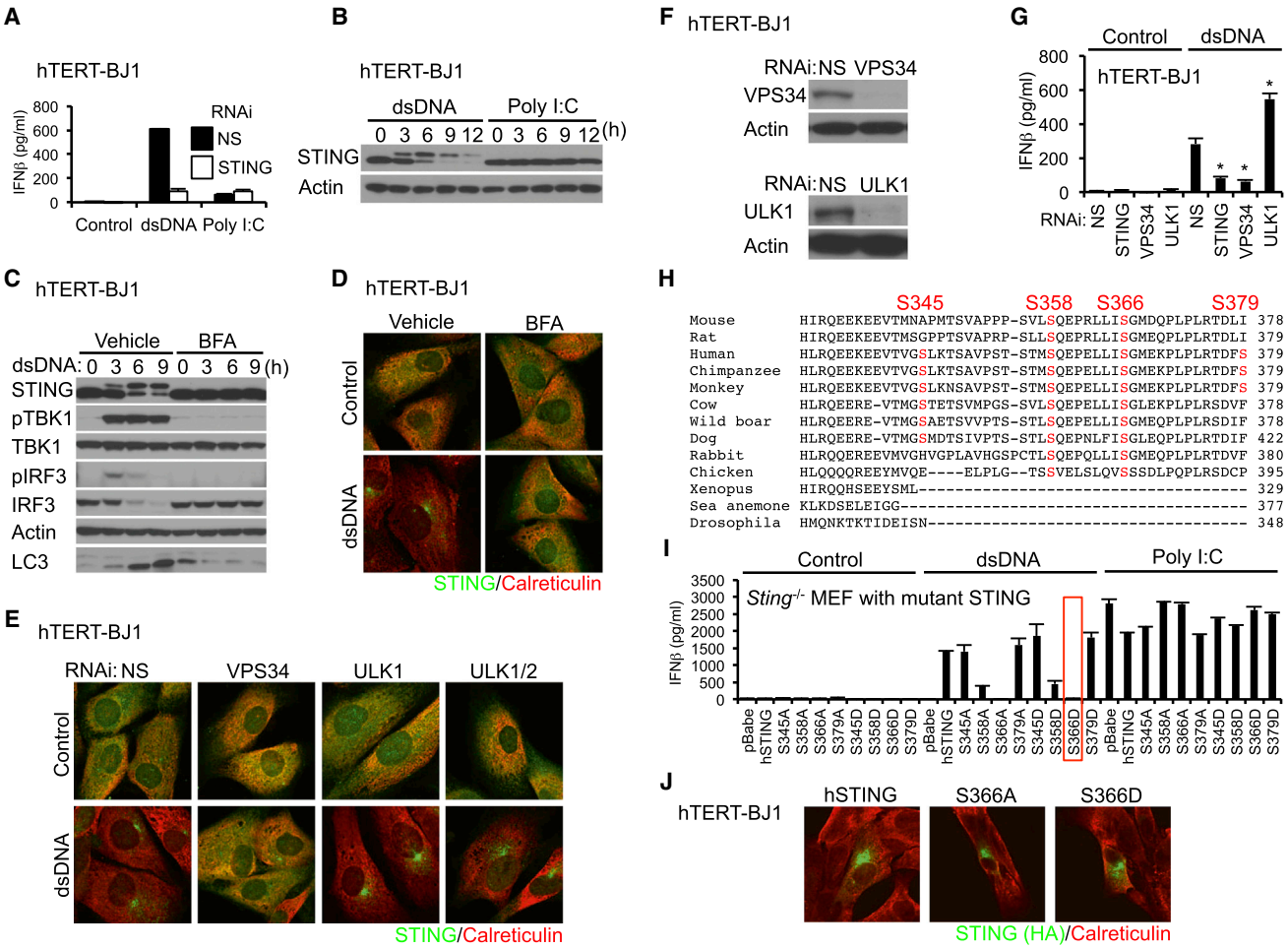

Figure 1. Phosphorylation of STING S366 Inhibits Type I IFN Production in dsDNA Signaling

(A) hTERT-BJ1 cells were transfected with dsDNA (4 μg/ml) or poly I:C (4 μg/ml) using lipofectamine 2000 for 16 hr. IFNβ level was measured by ELISA.

(B) hTERT-BJ1 cells were transfected with dsDNA or poly I:C as described in Figure 1A for the indicated times, and STING was detected by immunoblot.

(C and D) hTERT-BJ1 cells were incubated with ethanol (vehicle) or BFA (0.05 μg/ml) for 1 hr and then transfected with dsDNA (4 μg/ml) for the indicated times (C) or 6 hr (D). Immunoblot (C) or immunostaining (D) was performed with the indicated antibodies; lack of LC3 processing (bottom band) indicated loss of autophagy.

(E) hTERT-BJ1 cells were treated with siRNA (NS, nonspecific siRNA) for 3 days and then transfected with dsDNA (4 μg/ml) for 6 hr. Immunostaining was performed with the indicated antibodies.

(F) Immunoblot was performed to confirm knockdown efficiency of ULK1 and VPS34.

(G) siRNA-treated hTERT-BJ1 cells were transfected with dsDNA (4 μg/ml) for 16 hr, and IFNβ was measured by ELISA.

(H) Alignment of STING amino acid sequences. Highlighted amino acids indicate dsDNA-dependent phosphorylated serines, as detected by mass spectrometry.

(I) Primary *Sting*$^{-/-}$ MEF cells were reconstituted with STING variants using retroviruses. The cells were transfected with dsDNA (4 μg/ml) or poly I:C (4 μg/ml) for 16 hr, and IFNβ was measured by ELISA.

(J) hTERT-BJ1 cells were transfected with HA-tagged mutant hSTING for 36 hr and immunostained with the indicated antibodies.

Asterisks indicate significant difference ($p < 0.05$) compared to NS determined by Student's t test. Error bars indicate SD. See also Figure S1.

prolonged innate immune gene transcription and to prevent inflammatory disorders.

RESULTS

Phosphorylation of S366 Inhibits STING Function

Previously, we observed that STING activation by DNA invoked trafficking that resembled autophagy and resulted in the delivery of STING/TBK1 to endosomal/lysosomal regions to activate the transcription factors NF-κB and IRF3/7 (Ishikawa et al., 2009; Saitoh et al., 2009). As an extension of these findings, we have now determined that these events lead to an increase in the molecular weight of STING and subsequently to the degradation of STING within 12 hr (Figures 1A and 1B). The observed shift in molecular weight was likely due to phosphorylation because phosphatase treatment eliminated this modification (Figures S1A and S1B available online). Phosphorylation likely occurred after trafficking from the ER through the Golgi because Brefeldin A (BFA), which inhibited STING movement, also prevented the phosphorylation event (Figures 1C, 1D, and S1C). Degradation

of STING occurred in the lysosomal compartment because chloroquine, which inhibits lysosomal degradation, prevented STING degradation (Figure S1D). To further evaluate the autophagy process, we suppressed VPS34 (class III phosphatylinositol 3-kinase, PI3K), Beclin-1, or the serine/threonine protein kinase ULK1 (ATG1) expression, which are considered important components required for the autophagy process in response to nutrient deprivation (Tooze et al., 2010). We noted that RNAi suppression of VPS34, but not ULK1 or Beclin-1, inhibited STING trafficking, indicating ULK1-independent processes reminiscent of noncanonical autophagy reported for TLR9 activation in response to phagocytosed DNA associated with autoantibodies (Figures 1E, 1F, and S1E) (Henault et al., 2012). Accordingly, suppression of VPS34, but not ULK1, inhibited the ability of double-stranded DNA (dsDNA) to activate STING-dependent type I IFN induction (Figures 1F and 1G). Indeed, we observed that suppression of ULK1 appeared to augment the production of type I IFN. These observations indicate that STING recognition of dsDNA triggers a transient nonconventional autophagy-related process required for IRF3/7 and NF-κB activation.

However, after autophagy, little is known relating to the identity of kinases involved in STING phosphorylation and regulation. To start to evaluate the role of phosphorylation in STING function, we purified STING from dsDNA-treated and untreated hTERT-BJ1 cells using affinity purification processes. Nonactive STING or phosphorylated STING was examined by mass spectrometry. These experiments indicated that STING purified only from dsDNA-treated cells was phosphorylated in vivo on four sites (S345, S358, S366, and S379) (Figures 1H, S1F, and S1G). STING phosphorylation was not observed in resting, untreated cells (data not shown). Of the phosphorylation sites, S358 and S366 appeared to be highly conserved in mammalian cells (Figure 1H). To evaluate the role of these residues in STING function, each serine was individually or collectively substituted for alanine or aspartic acid and was transduced by retrovirus into *Sting*$^{-/-}$ MEFs prior to treatment with dsDNA. This analysis confirmed that S366A had greatly reduced ability to induce type I IFN (Figures 1I, S2A, and S2B) (Tanaka and Chen, 2012). However, we additionally observed that substitution of S366 to S366D to mimic constitutive phosphorylation also rendered STING unable to stimulate the production of type I IFN (Figure 1I). Substitution of the other serines to aspartic acid did not appreciably affect STING function except partially in the case of S358D. We further noted that S366A or S366D was able to traffic normally in response to cytosolic dsDNA, suggesting that phosphorylation of S366 does not affect STING trafficking and likely occurs post-Golgi trafficking (Figure 1J). We conclude that phosphorylation of S366 (S365 in murine STING) occurs after autophagy and may negatively regulate STING activity to prevent sustained type I IFN production following activation by cytosolic dsDNA.

The IRF3 Pathway, but Not the NF-κB Pathway, Is Preferentially Inhibited by STING S366D

Type I IFN production requires the coordinated activation of a number of transcription factors, such as NF-κB as well as IRF3 (Tamura et al., 2008). To evaluate whether both the IRF3 and the NF-κB pathways were affected by phosphorylation of S366, wild-type murine STING, STING-S365A, or STING-S365D were transfected into 293T cells with luciferase reporter constructs under control of IFNβ, NF-κB, or IRF3 (pRD III-I) responsive promoter elements. This study indicated that phosphomimetic STING-S365D failed to activate the IFNβ promoter and the IRF3 promoter, but not the NF-κB promoter (Figure 2A). Similarly, only STING variants with an S366 substitution failed to activate the pRD III-I promoter, but not the NF-κB promoter, indicating the importance of S366 in IRF3 stimulation (Figure 2B). The mutational change appeared to be S366 specific because residues substituted either side of S366 (I365A and G367A) did not influence STING function (Figure S2C). Accordingly, immunohistochemical analysis indicated the translocation of the p65 subunit of NF-κB, but not of IRF3, into the nucleus of *Sting*$^{-/-}$ MEF cells when reconstituted with S365D and treated with dsDNA (Figure 2C). STING is required to transport TBK1 to endosomal regions for association with IRF3 (Ishikawa et al., 2009). Immunoblot analysis of reconstituted *Sting*$^{-/-}$ MEF cells treated with dsDNA demonstrated TBK1 phosphorylation, but not phosphorylation of IRF3 (Figure 2D). Immunoblot analysis also indicated that murine S365D electrophoresed at a similar size to that of naturally phosphorylated STING, suggesting that the change in molecular weight occurring as a result of dsDNA activation was partly related to S365 phosphorylation (Figure 2D). Thus, S365 phosphorylation does not appear to affect TBK1 activity but rather affects IRF3 phosphorylation. To extend this analysis further, we stably reconstituted *Sting*$^{-/-}$ MEFs with wild-type STING or STING S365D and treated the cells with dsDNA before carrying out a microarray analysis. This analysis confirmed significant suppression of type I IFN production as well as other cytosolic DNA-mediated, STING-dependent genes, including members of the IFIT family (Figures 2E and 2F). However, the expression of a number of genes such as TNFAIP3 remained unaffected by phosphorylation of STING on S366 in the presence of cytosolic dsDNA, presumably because they only require NF-κB for transcriptional activation and not both IRF3/7 and NF-κB, as does the transcription of type I IFN (Figure 2G). Compared to the S365D variant, STING S365A was considerably more inactive, suggesting that the former does not simply function as a phosphomutant (Figure S2D). Our data confirm that phosphorylation of STING on S366 strongly prevents the transcriptional activity of IRF3.

ULK1 and 2 Are Responsible for Phosphorylating STING on S366

To attempt to identify the kinase responsible for phosphorylation of S366, we utilized a high-throughput approach and analyzed the ability of 272 purified serine/threonine kinases to in vitro phosphorylate a 9 amino acid peptide containing this residue (ELLISGMEK) (Figure 3A). We found that ULK1 and ULK2, key serine/threonine kinases involved in autophagy regulation, phosphorylated S366 to high specificity compared to all other kinases examined (17.1- and 21.13-fold respectively) (Mizushima, 2010). To confirm this finding, we carried out an in vitro kinase assay using purified STING and ULK1 and examined STING-related phosphorylation events by autoradiography following SDS-PAGE electrophoresis. Phosphorylation of STING was reduced

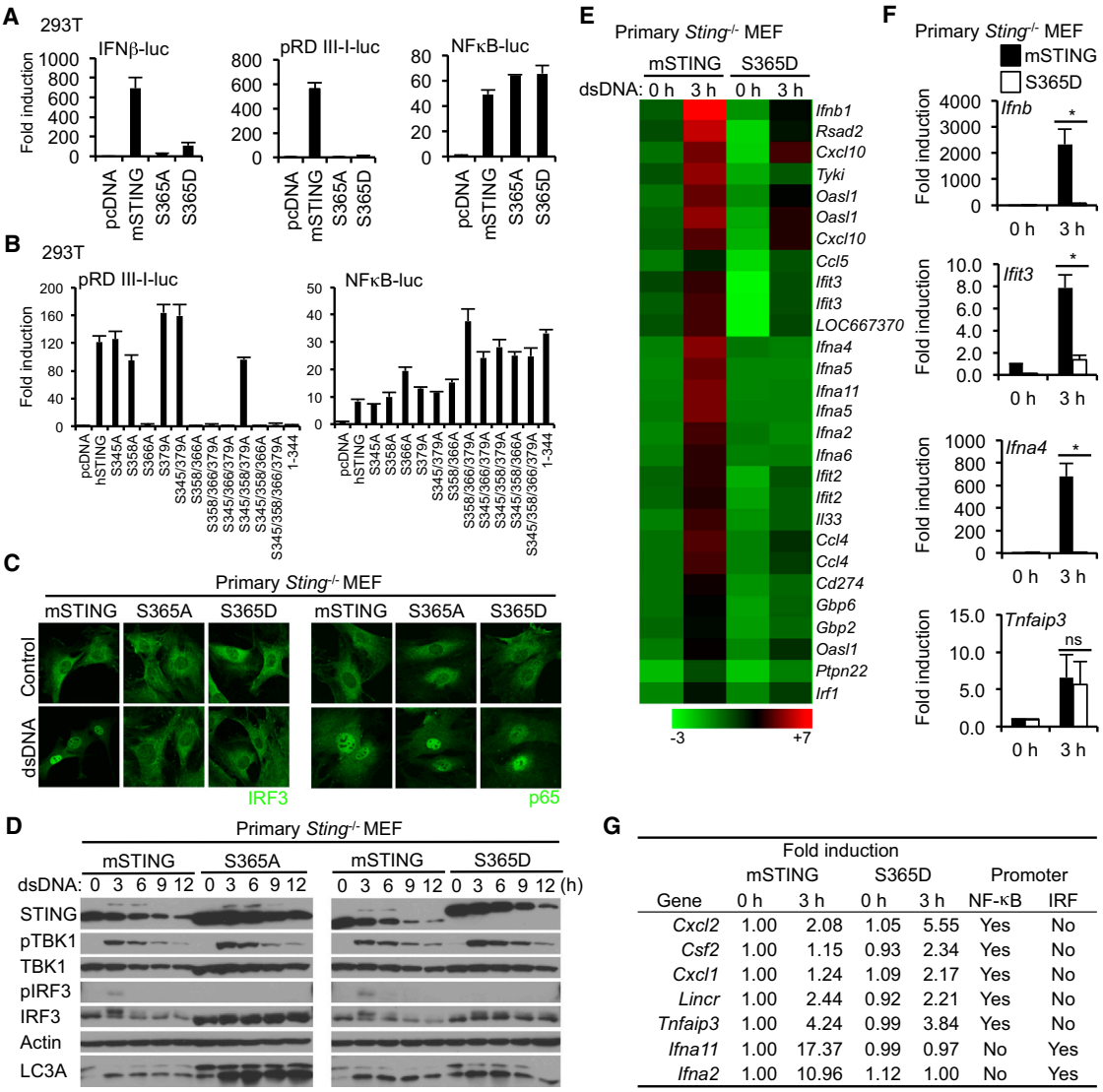

G

Gene	Fold induction mSTING 0 h	mSTING 3 h	S365D 0 h	S365D 3 h	Promoter NF-κB	Promoter IRF
Cxcl2	1.00	2.08	1.05	5.55	Yes	No
Csf2	1.00	1.15	0.93	2.34	Yes	No
Cxcl1	1.00	1.24	1.09	2.17	Yes	No
Lincr	1.00	2.44	0.92	2.21	Yes	No
Tnfaip3	1.00	4.24	0.99	3.84	Yes	No
Ifna11	1.00	17.37	0.99	0.97	No	Yes
Ifna2	1.00	10.96	1.12	1.00	No	Yes

Figure 2. Phosphorylation of S366 of STING Inhibits IRF3 Activity, but Not NF-κB Activity

(A and B) HEK293T cells were transfected with plasmids encoding the luciferase gene under control of the indicated promoter with STING variants. After 36 hr, luciferase activity was measured.

(C) Primary *Sting*$^{-/-}$ MEF cells were reconstituted with mSTING variants using retroviruses. The cells were transfected with dsDNA (4 μg/ml) for 3 hr and then stained with the indicated antibodies.

(D) Reconstituted *Sting*$^{-/-}$ MEF cells were transfected with dsDNA (4 μg/ml) for the indicated times, and immunoblots were performed.

(E) Reconstituted *Sting*$^{-/-}$ MEF cells were transfected with dsDNA (4 μg/ml) for 3 hr. RNA was purified and examined for gene expression with Illumina Sentrix BeadChip Array (Mouse WG6 version2). Pseudocolors indicate transcript levels below, equal to, or above the mean (green, black, and red, respectively). The scale represents the intensity of gene expression (log10 scale). The results shown here are representative of three independent experiments.

(F) Real-time PCR was carried out with the indicated probes to confirm gene array analysis shown in Figure 2E. Total RNA was extracted from reconstituted *Sting*$^{-/-}$ MEF cells after dsDNA treatment for 3 hr, and then cDNA was synthesized.

(G) The expression of NF-κB target genes in *Sting*$^{-/-}$ MEF with S365D was comparable with that in *Sting*$^{-/-}$ MEF with mSTING. Promoter sequence of listed genes (−1,000 to +200) was obtained through DBTSS (http://dbtss.hgc.jp) and analyzed by TFSEARCH (http://www.cbrc.jp/research/db/TFSEARCH.html) at threshold score 85. The results shown here are the averages of three independent experiments.

Asterisks indicate significant difference ($p < 0.05$) determined by Student's t test. ns means not significant. Error bars indicate SD. See also Figure S2.

using a STING S336A variant (Figures 3B and 3C). To additionally verify this, we isolated ULK1-phosphorylated STING from SDS-PAGE gels and determined the phosphorylation site(s) by mass spectrometry. This approach confirmed phosphorylation of STING by ULK1 and additionally demonstrated that this event only occurred on S366 and on no other serine or threonine residues (Figure 3D). As a control, we similarly examined the ability of TBK1 to posttranslationally modify STING and did not

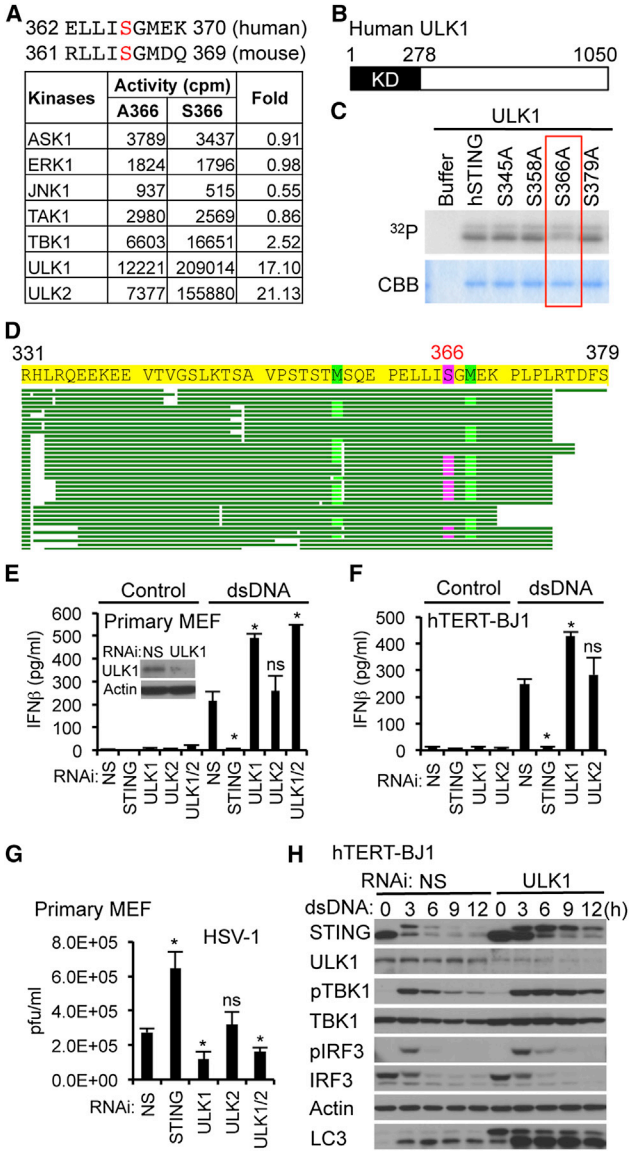

Figure 3. ULK1 Negatively Regulates IFNβ Production by Phosphorylating STING S366

(A) ELLISGMEK, which includes Ser366, was used as substrate to identify ULK1 and ULK2.

(B) Schematic of human ULK1. KD is kinase domain.

(C) In vitro kinase assay was performed with recombinant ULK1 protein using recombinant hSTING protein as substrate. The indicated serine sites that were identified by mass spectrometry were substituted with alanine.

(D) Recombinant hSTING protein was incubated with recombinant ULK1 in the presence of ATP for 15 min. Phosphorylated STING was analyzed by mass spectrometry. Highlighted amino acid (S366) was identified as the only phosphorylation site.

(E and F) Primary MEF cells (E) or hTERT-BJ1 cells (F) were treated with siRNA as indicated (NS, nonspecific siRNA) and then transfected with dsDNA (4 μg/ml) for 16 hr. IFNβ was measured by ELISA. Knockdown efficiency of ULK1 in primary MEF cells was confirmed by immunoblot.

(G) siRNA-treated primary MEF cells were infected with HSV-1 (MOI = 0.1) for 24 hr, and then plaque assay was performed.

(H) siRNA-treated hTERT-BJ1 cells were transfected with dsDNA (4 μg/ml) for the indicated times, and then immunoblot was performed.

observe any phosphorylation events, indicating that STING is likely not a substrate for TBK1, at least in vitro (Figures S3A–S3C). Collectively, these data indicate that ULK1/2 can phosphorylate STING on S366.

To evaluate these findings further, we RNAi suppressed ULK1, ULK2, or both in MEF cells treated with dsDNA and measured type I IFN production. We found, using MEF cells, that suppression of STING expression significantly abrogated IFN production in response to dsDNA signaling and confirmed that ULK1 suppression lead to elevated levels of type I IFN production presumably because IRF3 function is maintained (Figure 3E). Similar observations were seen when suppressing ULK1 expression in hTERT-BJ1 cells (Figure 3F). Suppression of ULK2 had less effect, probably because we did not observe significant ULK2 expression, at least in hTERT-BJ1 or MEF cells (Figures S3D and S3E). ULK1 and 2 were also observed to be robustly expressed in primary human dendritic cells (Figure S3F). Suppression of ULK1 expression in MEF cells was also seen to inhibit herpes simplex virus type I (HSV1) replication, likely due to elevated type I IFN exerting antiviral effects (Figures 3G and S3G). Immunoblot analysis of ULK1-specific RNAi-treated hTERT-BJ1 cells indicated that STING was not degraded as efficiently as in control cells, suggesting that phosphorylation on this site may also play a role in facilitating STING degradation (Figure 3H). STING also shifted in size due to alternate phosphorylation events, plausibly involving the other three serine sites that we discovered by proteomic approaches (Figure 1H). Slightly sustained TBK1 and IRF3 phosphorylation was also observed in the absence of ULK1, perhaps indicating that the presence of STING facilitates TBK1 stability. As shown earlier, loss of ULK1 did not affect STING-dependent autophagy, as additionally emphasized by evident LC3-II conversion (Figures 1C and 3H). Our data indicate that ULK1 and perhaps ULK2, depending on whether a particular cell expresses ULK2, are able to phosphorylate STING on S366 to perhaps facilitate STING degradation as well as prevent IRF3 translocation.

AMPK, Not mTOR, Is the Master Regulator of ULK1/2 Activity

The mechanisms whereby ULK1 is regulated are complex though are known to involve control by AMPK and mammalian target of rapamycin (mTOR) (Alers et al., 2012). AMPK is a heterotrimeric protein and key energy-sensing kinase that is activated by environmental stress such as Ca^{2+} efflux or ATP consumption. Under nonstressful conditions, AMPK T172 is maintained in a phosphorylated state by upstream AMPK kinases such as LKB1 and Ca^{2+}-calmodulin dependent protein kinase-kinase-β (CaMKK β) (Alexander and Walker, 2011). Constitutively phosphorylated AMPK in turn phosphorylates ULK1 on S556, which maintains ULK1 in an inactive state. However, additional posttranslational modifications of AMPK following cell stress releases it from association with ULK1 with concomitant loss

Asterisks indicate significant difference ($p < 0.05$) compared to NS determined by Student's t test. ns, not significant. Error bars indicate SD. See also Figure S3.

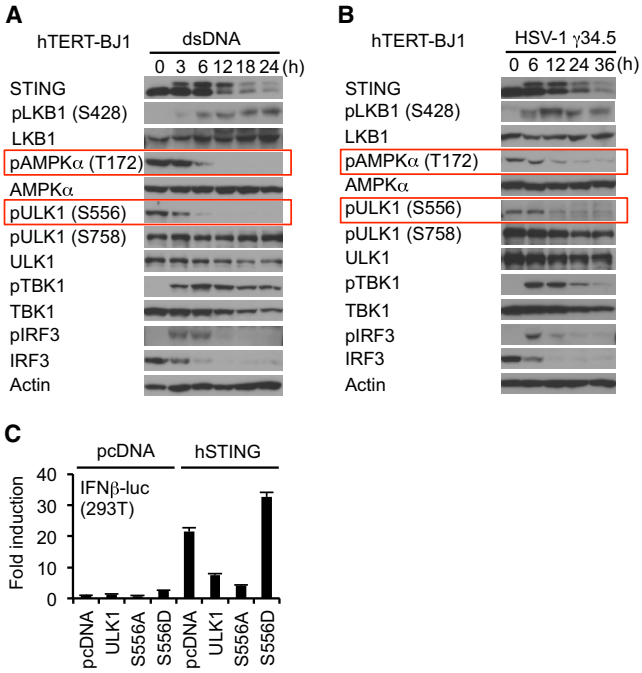

Figure 4. dsDNA Induces the Dephosphorylation of AMPK T172 and ULK1 S556

(A and B) hTERT-BJ1 cells were transfected with dsDNA (4 μg/ml) (A) or infected with HSV-1 γ34.5 (MOI = 10) (B) for the indicated times, and then immunoblot was carried out with the indicated antibodies.

(C) HEK293T cells were cotransfected with plasmids encoding luciferase driven by the IFNβ promoter as well as hSTING and ULK1 variants. After 36 hr, luciferase activity was measured.

Error bars indicate SD. See also Figure S4.

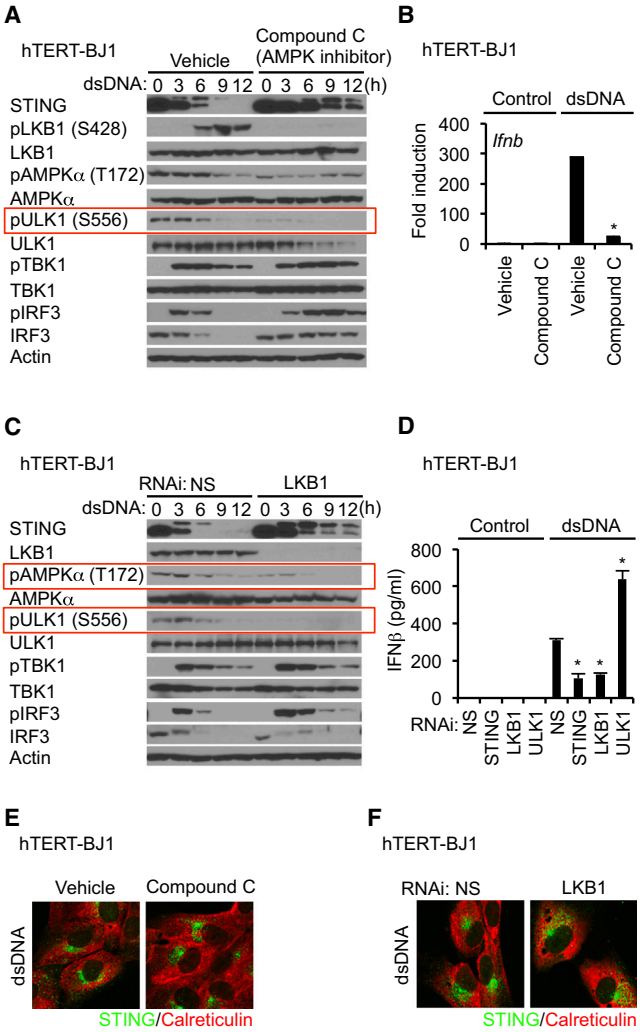

Figure 5. LKB1 Phosphorylation of AMPK Is Disrupted by Cytosolic dsDNA

(A) hTERT-BJ1 cells were treated with DMSO (vehicle) or compound C (10 μM) for 1 hr prior to dsDNA transfection (4 μg/ml) for the indicated times. Immunoblot was performed with the indicated antibodies.

(B) hTERT-BJ1 cells were treated with DMSO or compound C as described in Figure 5A and then transfected with dsDNA (4 μg/ml) for 6 hr. cDNA was synthesized from total RNA, and then real-time PCR was performed with a probe for *Ifnb*.

(C) hTERT-BJ1 cells were treated with siRNA for NS (nonspecific siRNA) or LKB1 and then transfected with dsDNA (4 μg/ml) for the indicated times. Immunoblot was performed with the indicated antibodies.

(D) siRNA-treated hTERT-BJ1 cells were transfected with dsDNA (4 μg/ml) for 16 hr. IFNβ was measured by ELISA.

(E and F) hTERT-BJ1 cells were treated with compound C as described in Figure 5A (E) or siRNA for LKB1 as described in Figure 5C (F). Confocal analysis of STING trafficking in response to dsDNA (4 μg/ml) was carried out using anti-STING antibody.

Asterisks indicate significant difference ($p < 0.05$) compared to vehicle (B) or NS (D) determined by Student's t test. Error bars indicate SD. See also Figure S5.

of ULK1 S556 phosphorylation (Alers et al., 2012). This enables ULK1 to phosphorylate target proteins. Similarly, mTOR, which can be activated by amino acid deprivation, likewise regulates ULK1 activity through phosphorylation but targets S758 (Mizushima, 2010). Given this, we examined the control of ULK1 phosphorylation by these two pathways. When treated with dsDNA, we noted that phosphorylation of ULK1 S758 was relatively unaffected following dsDNA treatment (Figure 4A). However, we observed that phosphorylation of AMPKα T172 was dramatically reduced in the presence of cytosolic DNA, which corresponded to a reduction of S556 on ULK1 (Figure 4A). The effect induced by dsDNA was also seen following infection with HSV1 (Figure 4B). In contrast, vesicular stomatitis virus (VSV) did not induce dephosphorylation of AMPK T172 or ULK1 S556 (Figure S4A). Constitutively active ULK1 (S556D) was observed to enhance the ability of STING to stimulate transcription of the IFN promoter, unlike ULK1 S556A, presumably because ULK1 S556D is maintained in an inactive, phosphorylated state, which fails to impede IRF3 function (Figure 4C). The kinase activity of ULK1 was confirmed to be required for the regulation of STING (Figure S4B). Inhibition of AMPK by compound C substantiated that ULK1 S556 phosphorylation was an AMPK-dependent event because this process was completely negated by this drug (Figure 5A). Accordingly, compound C thus

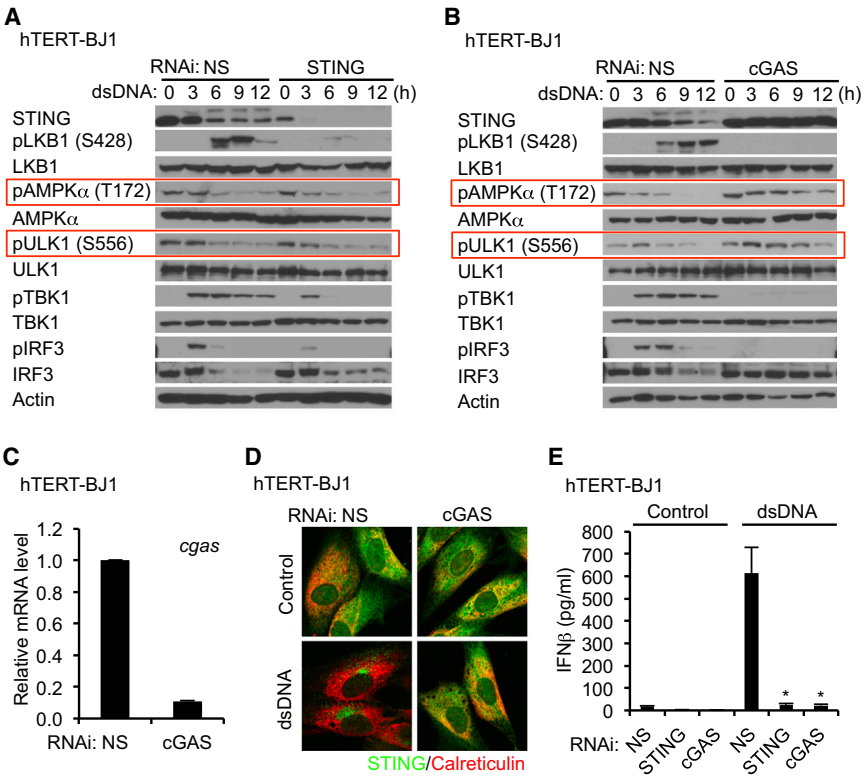

Figure 6. cGAS Is Required for the Negative Regulation of STING through the AMPK-ULK1 Axis

(A and B) hTERT-BJ1 cells were treated with siRNA for NS (nonspecific), STING (A), and cGAS (B) for 3 days and then transfected with dsDNA (4 μg/ml) for the indicated times. Immunoblot was performed with the indicated antibodies.

(C) Knockdown efficiency of cGAS in hTERT-BJ1 cells was confirmed by real-time PCR.

(D) siRNA-treated hTERT-BJ1 cells were transfected with dsDNA for 6 hr as described in Figure 6A. STING trafficking was observed by confocal microscopy.

(E) siRNA-treated hTERT-BJ1 cells were transfected with dsDNA (4 μg/ml) for 16 hr. IFNβ was measured by ELISA.

Asterisks indicate significant difference ($p < 0.05$) compared to NS determined by Student's t test. Error bars indicate SD. See also Figure S6.

suppressed dsDNA-dependent, but not significantly dsRNA-dependent type I IFN, induction (Figures 5A, 5B, and S5A). We observed that AMPK inhibition facilitated STING stability, similar to loss of ULK1, again indicating that phosphorylation of STING affects its degradation (Figure 5A). Moreover, levels of IRF3 were maintained and did not undergo rapid degradation, presumably because phosphorylated IRF3 did not translocate and was not efficiently degraded (Figures 5A and S5B). Conversely, activation of AMPK was also seen to modestly enhance type I IFN production (Figure S6D).

Given these findings, we next evaluated the roles of the AMPK kinases, CaMKK β and LKB1 in cytosolic dsDNA signaling. We observed that suppression of CaMKK β somewhat reduced the phosphorylation status of AMPK T172, but ULK1 S556 phosphorylation was maintained under resting conditions and underwent dephosphorylation in the presence of cytosolic DNA, suggesting that a kinase other than CaMKK β may be predominantly involved in the regulation of AMPK T172 (Figures S5D and S5E). In addition, we noted that cytosolic DNA also induced the phosphorylation of LKB1 on S428 and that this was also dependent on AMPK (Figures 5A and S5C). To further investigate the role of LKB1 in AMPK/ULK1 activity, we used RNAi to suppress LKB1 expression. Loss of LKB1 completely eliminated ULK1 S556 phosphorylation under resting conditions, indicating that LKB1 was largely responsible for maintaining AMPK T172 phosphorylation and for limiting ULK1 activity (Figure 5C). Loss of LKB1 was also observed to inhibit dsDNA-dependent type I IFN induction, similar to compound C (Figure 5D). These events were predominantly dsDNA specific and did not occur using lipofectamine alone (Figure S5F). It was also observed that loss of LKB1 or AMPK activity did not affect STING autophagy, suggesting that AMPK control of ULK1 occurs in autophagosome/endosomal regions after STING trafficking (Figures 5E and 5F). Our data indicate that LKB1 predominantly maintains phosphorylation of AMPK on T172, an event that is disrupted by the presence of cytosolic DNA, leading to ULK1 activation and STING phosphorylation.

cGAMPs Regulate AMPK

The activation of AMPK has been reported to be dependent on nutrient deprivation, fluctuations in calcium levels, and/or increases in AMP/ATP ratios. However, we did not notice significant fluctuations in the levels of these regulators (data not shown). We also observed that loss of STING in hTERT-BJ1 cells did not affect the phosphorylation of AMPK on T172 or ULK1 on S556, indicating that the control of ULK1 phosphorylation by cytosolic DNA was a STING-independent event (Figure 6A). However, loss of STING impeded cytosolic DNA-mediated autophagy and prevented LKB1 phosphorylation by AMPK on S428. BFA also prevented LKB1 phosphorylation by AMPK by similarly impeding autophagy-related trafficking (Figure S6A). We confirmed that, although STING was required for cytosolic DNA-mediated autophagy, it was not necessary for rapamycin-dependent autophagy (Figure S6B).

To further understand the triggering of AMPK/ULK1 activity, we used RNAi to suppress the synthase cGAS, which has been reported to associate with cytoplasmic DNA and to generate cyclic dinucleotides that are capable of binding to and facilitating STING function. Surprisingly, we observed that loss of cGAS prevented AMPK T172 dephosphorylation and, subsequently, ULK1 S566 dephosphorylation (Figures 6B and 6C). STING-dependent autophagy was also prevented by loss of cGAS in hTERT-BJ1 cells, in response to dsDNA

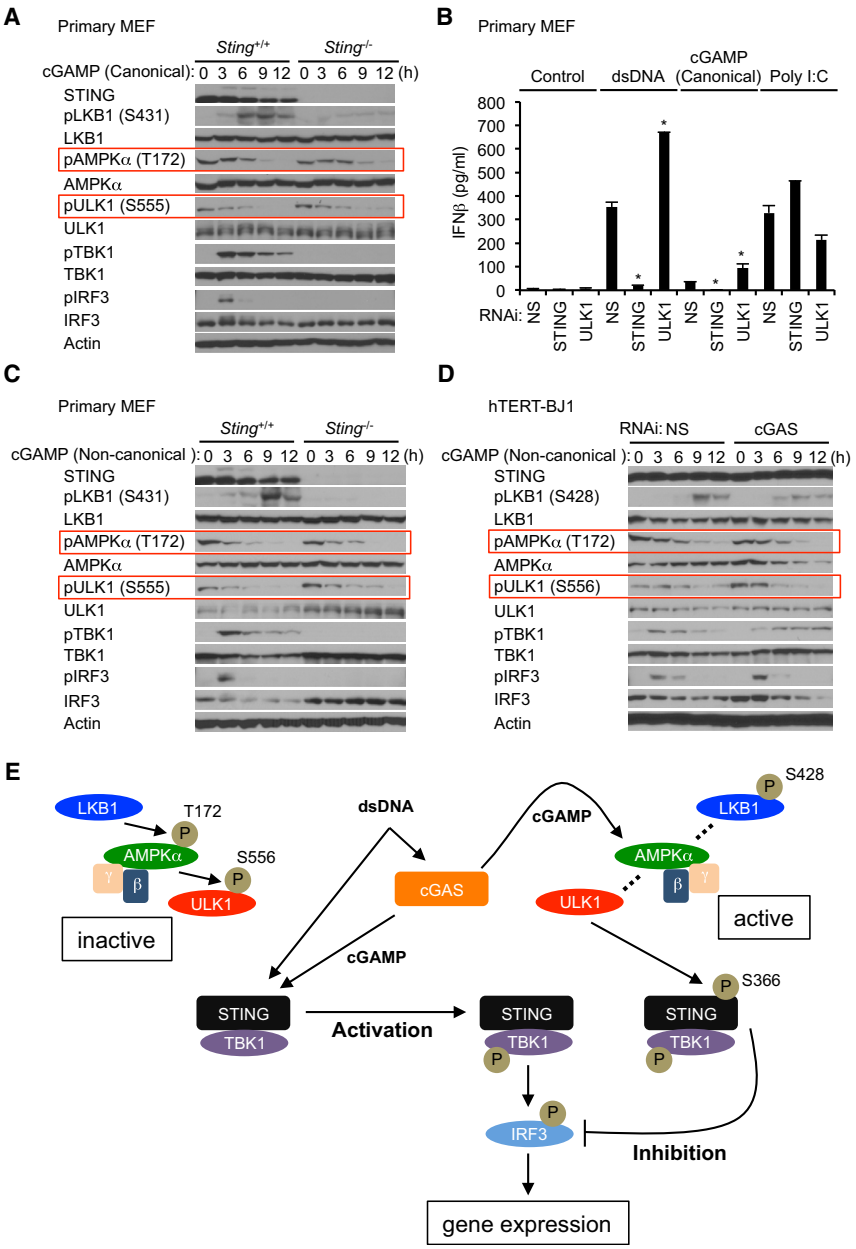

Figure 7. cGAMPs Activate AMPK-ULK1 Control of STING

(A) Primary *Sting*$^{+/+}$ and *Sting*$^{-/-}$ MEF cells were transfected with canonical cGAMP (3′ to 5′ cGAMP) (8 μg/ml) using lipofectamine 2000 for the indicated times. Immunoblot was performed with the indicated antibodies.

(B) Primary MEF cells were treated with siRNA for NS (nonspecific), STING, or ULK1 for 3 days and then transfected with dsDNA (4 μg/ml), canonical cGAMP (8 μg/ml), or poly I:C (4 μg/ml) as described in Figure 7A for 16 hr. IFNβ was measured by ELISA.

(C) Primary *Sting*$^{+/+}$ and *Sting*$^{-/-}$ MEF cells were transfected with noncanonical cGAMP (2′ to 5′ cGAMP) (8 μg/ml) as described in Figure 7A for the indicated times. Western blot was performed with the indicated antibodies.

(D) hTERT-BJ1 cells were treated with siRNA for NS or cGAS for 3 days and then transfected with noncanonical cGAMP (8 μg/ml) as described in Figure 7A for the indicated times. Immunoblot was performed with the indicated antibodies.

(E) Model of STING activation by cytosolic DNA and subsequent inhibition by ULK1.

Asterisks indicate significant difference ($p < 0.05$) compared to NS determined by Student's t test. Error bars indicate SD. See also Figure S6.

(Figures 6D and 6E). These results suggested a role for cGAS and the generation of cyclic dinucleotides in the regulation of AMPK activity. To extend our studies, we next examined whether cGAMP could activate the AMPK/ULK1 pathway in mouse embryonic fibroblast (MEF) cells. This analysis confirmed that canonical and noncanonical cGAMP alone could trigger the dephosphorylation of AMPK and ULK1 on T172 and S555, respectively (Figures 7A–7C). This event did not require STING, as previously shown (Figures 6A and 7A). Similar to our observations with dsDNA, loss of ULK1 enhanced cGAMP's ability to induce type I IFN. However, we notice that cyclic dinucleotides are not as robust activators of STING-dependent innate immune signaling when compared to dsDNA (Figure 7B). We next treated hTERT-BJ1 cells with noncanonical cGAMP to evaluate whether these dinucleotides could similarly activate the AMPK/ULK1 regulatory pathway. In hTERT-BJ1 cells, the amino acid sequence of STING is H232, which cannot bind readily to canonical cyclic dinucleotides such as c-di-AMP, c-di-GMP, or cGAMP (Ablasser et al., 2013; Civril et al., 2013; Gao et al., 2013; Kranzusch et al., 2013; Zhang et al., 2013). In most other types of human cells, such as THP-1, the amino acid sequence of STING is R232, which can bind readily to canonical cyclic dinucleotides. This analysis demonstrated that, comparable to MEF cells, noncanonical cGAMP triggered the dephosphorylation of AMPK T172 and ULK1 S556 in hTERT-BJ1 cells (Figure 7D). In addition, noncanonical cGAMP also stimulated the phosphorylation of TBK1 and IRF3 in hTERT-BJ1 cells, albeit weaker than in comparison with dsDNA (Figure 7D). Noncanonical cGAMP was observed to induce STING trafficking in both primary MEF cells and hTERT-BJ1 cells, whereas canonical cGAMP activated STING only in MEF cells (Figure S6C). Collectively, our data indicate that cGAS is essential for the activation of AMPK/ULK1 suppression of STING (Figure 6B) and that cGAMPs are responsible for triggering the dephosphorylation of AMPK T172 and activation of ULK1, which phosphorylates STING on S366 to impede its activity (Figure 7E). Thus, cyclic dinucleotides, although facilitating STING function, provide a means to control STING via a negative-feedback loop.

DISCUSSION

Our data demonstrate that, in the presence of cytosolic DNA, STING rapidly traffics with TBK1 via VPS34-related autophagosomes to associate with endosomal compartments containing NF-κB and IRF3. This triggers the production of numerous cytokines and chemokines that can regulate the adaptive immune response (Abe et al., 2013; Ishikawa and Barber, 2008; Ishikawa et al., 2009). This event appears to be independent of ULK1 and is reminiscent of a noncanonical autophagy-related process involving plasmacytoid dendritic cell (pDC)-mediated phagocytosis of antinuclear antibody bound to CpG DNA (DNA-immune complexes, DNA-IC) (Henault et al., 2012). Following DNA-IC engulfment, autophagy facilitates DNA-dependent TLR9 trafficking to cellular compartments harboring IRF3 and NF-κB. Our data here indicate a similar mechanism of type I IFN induction that is dependent on STING and that is triggered by non-CpG DNA species. Aside from being ULK1 independent, STING-dependent autophagosomes do not have double-membrane structures and are dependent on ATG9a (Ishikawa et al., 2009; Saitoh et al., 2009). After trafficking, STING is phosphorylated and degraded, presumably to avoid the deleterious consequences that sustained innate immune gene induction can have upon the host (Ahn et al., 2012). Our data here indicate that the phosphorylation of STING occurs after the formation of autophagosomes and trafficking through the Golgi and predominantly occurs on four serine residues as determined by mass spectrophotometry. Subsequent studies indicated that phosphorylation of S366 was found to inhibit STING-dependent IRF3 activity, but not robustly NF-κB. Indeed, the mechanisms whereby STING controls NF-κB activity remain to be determined. We note that phosphorylation of S366 may also facilitate STING degradation to additionally prevent sustained function. It is not clear why the three remaining serine sites are targeted for phosphorylation. However, our data suggest that they do not strongly affect STING function but more likely influence STING turnover to ensure that the presence of STING is not lasting. It was also noted that STING longevity (for example, achieved by expression of STING S366A that could not be phosphorylated or suppression of ULK1) corresponded with a decrease in the degradation of phosphorylated TBK1. Thus, STING appears to be phosphorylated in autophagosome/endosomal compartments and degraded, a consequence that enables the proteolytic degradation of phosphorylated TBK1 after it has phosphorylated IRF3. A STING variant (S366A), unable to be phosphorylated, in contrast appears to shield TBK1 from degradation and to largely prevent the phosphorylation and translocation of IRF3 by mechanisms that remain to be clarified. However, it is possible that phosphorylated TBK1 may require release from STING to be able to target IRF3. The mechanisms of how STING/VPS34 preautophagosomal structures (PAS) are initiated are also unknown and will be the focus of further study.

Using a serine/threonine kinase library, we determined that, after trafficking, STING S366 was predominantly phosphorylated by the mammalian *C. elegans* uncoordinated-51 (UNC-51)-like kinase ULK1 (ATG1) and ULK2, first identified as important components of the autophagy process in yeast (Alers et al., 2012; Mizushima, 2010; Tooze et al., 2010). Mammalian ULK1 shares ~50% homology with ULK2, and the loss of both completely blocks amino acid starvation-induced autophagy in murine embryonic fibroblasts (Alers et al., 2012). ULK1 appears to be more ubiquitously expressed than ULK2 and exists in a complex with ATG13 and RB1CC1. The major energy sensor, MTOR, as a complex with RAPTOR and MLST8 (MTOR complex 1; MTORC1), directly phosphorylates ULK1 on S758 under nutrient-rich conditions, an event that likely sequesters ULK1 in an inactive state through association with RAPTOR. Inhibition of the MTOR complex by rapamycin, for example, is sufficient to induce autophagy (Alers et al., 2012; Mizushima, 2010). However, we did not see any dephosphorylation of ULK1 S758 in cytosolic DNA-treated cells. Moreover, rapamycin-dependent autophagy was observed to occur independently of STING, unlike cytosolic DNA-mediated autophagy, which did require STING. In contrast, we did observe dephosphorylation— which is controlled by another key energy sensor, AMPK—of ULK1 S556 in hTERT-BJ1 and MEF cells (Hardie et al., 2012). In this situation, AMPK, which exists as a heterotrimeric protein (α, β, γ) can be targeted by a number of kinases such as CaMKK β, which responds to fluctuations in calcium levels, or by liver kinase B1 (LKB1; also referred to as serine/threonine kinase 11, STK11), which responds to fluctuations in ADP and AMP. LKB1 similarly exists in a trimeric complex with the pseudokinase STRAD and the adaptor protein MO25 (Alexander and Walker, 2011). Phosphorylation of AMPK by CaMMK β or LKB1 causes the dephosphorylation of T172 and prevents AMPK from phosphorylating ULK1 on S556. However, our data indicated that, in response to cytosolic DNA, relatively low fluctuations in Ca^{2+} or AMP levels were measurable, suggesting that other modes of AMPK T172 dephosphorylation were responsible. Nevertheless, we did note that LKB1 was essential for AMPK phosphorylation on T172. This leads us to consider alternate mechanisms of LKB1/AMPK/ULK1 control and to investigate the role of cyclic dinucleotides in this process. First, we found a key role for the synthase cGAS in AMPK dephosphorylation in response to cytosolic DNA. Concomitantly, we observed that canonical or noncanonical cyclic dinucleotides can themselves directly cause the dephosphorylation of AMPK T172 and ULK1 S556 in a STING or cGAS-independent manner. Thus, cGAS is likely responsible for generating cyclic dinucleotides from cytosolic DNA, which facilitates STING activity. In addition, cGAS-generated cGAMPs provide a mechanism for the subsequent negative control of STING that occurs after trafficking and delivery of TBK1 to cellular compartments containing IRF3 and NF-κB. It is not yet clear how cyclic dinucleotides activate the LKB1/AMPK/ULK1 axis. However, the cyclic nucleotide cAMP has been reported to regulate the Epac (exchange protein directly activated by cAMP) family, which are guanine nucleotide exchange factors (GEFs) able to influence LKB1-mediated control of AMPK T172 phosphorylation (Fu et al., 2011). Relatively few cyclic dinucleotide-binding proteins have thus far been reported, and so the identification of the cGAMP regulators of AMPK activity remains to elucidated. In summary, cyclic dinucleotide control of AMPK/ULK1 and STING helps ensure that sustained production of STING-dependent proinflammatory genes is prevented, events that may otherwise lead to inflammation

and autoimmune disorders (Ahn et al., 2012; Gall et al., 2012). Our data provide information on the control of DNA-mediated innate immune signaling pathways that could conceivably be therapeutically targeted to help prevent a variety of self-DNA-triggered disorders.

EXPERIMENTAL PROCEDURES

Cells, Reagents, and Viruses

Primary *Sting*$^{+/+}$ and *Sting*$^{-/-}$ MEF cells were prepared as described (Ishikawa and Barber, 2008). *Tbk1*$^{-/-}$ MEF cells were kindly provided by W.C. Yeh. HEK293T cells, Platinum-E retroviral packaging cell line, hTERT-BJ1 cells, and primary human dendritic cells were purchased from the American Type Cell culture (ATCC), Cell Biolabs, Clontech, and Stemcell, respectively. MEF cells, HEK293T cells, and Platinum-E cells were cultured in DMEM supplemented with 10% FBS and antibiotics. hTERT-BJ1 cells were cultured in a 4:1 ratio of DMEM: Medium 199 with 10% FBS, 1 mM sodium pyruvate, and 4 mM L-glutamine. Poly I:C was obtained from American Biosciences. Interferon stimulatory DNA (ISD) (90-mer), used as dsDNA in this study, was prepared as described previously (Ishikawa and Barber, 2008). Canonical cGAMP (3′ to 5′ cGAMP) and noncanonical cGAMP (2′ to 5′ cGAMP) were purchased from Invivogen and BioLog, respectively. BFA, compound C, rapamycin, and STO-609 were purchased from SIGMA. Nonspecific siRNA (NS), siRNA for STING, ULK1, ULK2, LKB1, cGAS, VPS34, and Beclin-1 were purchased from Dharmacon. Lipofectamine 2000 and lipofectamine RNAiMAX were purchased from Invitrogen. Anti-STING rabbit polyclonal antibody was prepared as described previously (Ishikawa and Barber, 2008). Other antibodies used in this paper were as follows: anti-β-actin (SIGMA, A5441); anti-calreticulin (Abcam, ab14234); anti-IRF3 (Invitrogen, 39-2700, used for murine IRF3); anti-IRF3 (Santa Cruz Biotechnology, sc-9082); anti-phospho-IRF3 (Cell Signaling, 4947); anti-p65 (Cell Signaling, 3987); anti-TBK1 (Abcam, ab40676); anti-phospho-TBK1 (Cell Signaling, 5483); anti-LC3A (Cell Signaling, 4599); anti-ULK1 (Cell Signaling, 4773); anti-phospho-ULK1 (Ser556) (Cell Signaling, 5869); anti-phospho-ULK1 (Ser758) (Cell Signaling, 6888); anti-ULK2 (Abcam, ab97695); anti-AMPKα (Cell Signaling, 5832); anti-phospho-AMPKα (Thr172) (Cell Signaling, 2535); anti-VPS34 (Cell Signaling, 4263); anti-Beclin-1 (Cell Signaling, 3495); anti-LKB1 (Cell Signaling, 3047); anti-phospho LKB1 (Ser428) (Abcam, ab63473); and anti-HA (SIGMA, H9658). HSV-1 (KOS strain) was purchased from ATCC. HSV-1 γ34.5 was kindly provided by Bernard Roizman. HSV-1 luc was kindly provided by David Leib. Purified ULK1 and TBK1 were purchased from SIGMA and Millipore, respectively. Probe for *Ulk1*, *Ulk2*, *Infb*, *Ifit3*, *Ifna4*, *Tnfaip3*, and *cgas* was purchased from Applied Biosystems.

Proteomics

hTERT-BJ1 cells in ten 15 cm dishes were used for untreated samples, dsDNA-treated samples, and negative controls (untreated and precipitated with mouse IgG), respectively. The cells were transfected with 5 μg/ml of dsDNA for 6 hr. After that, the cells were lysed in TNE buffer (50 mM Tris [pH 7.5], 150 mM NaCl, 1 mM EDTA, 1% NP-40) with protease and phosphatase inhibitors and then subjected to immunoprecipitation with monoclonal anti-STING antibody covalently conjugated beads for 18 hr at 4°C. After washing with TNE buffer, STING protein was eluted using Elution buffer (pH 2.8, Thermo) and then neutralized by Tris-HCl (pH 9.5). The samples were boiled in SDS-sample buffer and then separated in a 7.5% acrylamide gel. The gel was stained with CBB staining kit (Thermo), and the visualized bands, including STING, were analyzed by microcapillary reverse-phase HPLC nanoelectrospray tandem mass spectrometry (μLC/MS/MS) at the Harvard Mass Spectrometry and Proteomics Resource Laboratory.

Reconstitution of *Sting*$^{-/-}$ MEF Cells

Platinum-E retroviral packaging cells were transfected with pBabe-STING-puro using Lipofectamine 2000. After 2 days, the supernatants containing retrovirus were collected. *Sting*$^{-/-}$ MEF cells were incubated with the supernatants in the presence of 10 μg/ml of polybrene (SIGMA) for 6 hr. After another 2 days, 2 μg/ml of puromycin (SIGMA) was added to culture media to remove uninfected cells.

In Vitro Kinase Assay

181–379 of hSTING was cloned into pET-26b and expressed in BL21 (DE3). Recombinant hSTING protein was isolated using HisPur Ni-NTA Resin (Thermo) and eluted with imidazole. 60 ng of hSTING protein was incubated with 20 ng of GST-ULK1 in 20 mM Tris-HCl (pH 7.5), 25 mM KCl, 0.1 mM EDTA, 1 mM DTT, 5% glycerol, 2 mM $MgCl_2$, 2 mM $MnCl_2$, 1.25 μM ATP, and 0.3 mg/ml BSA in presence of [γ-^{32}P] ATP (Perkin Elmer) for 15 min at 30°C. The samples were boiled in SDS-sample buffer and separated in a 7.5% acrylamide gel. After running the gel, gel was fixed in 40% methanol solution with 10% acetic acid and stained with CBB staining kit (Thermo). After destaining, the dried gel was exposed to BioMax Light Film (Kodak).

Kinase Screening

To identify the kinase that phosphorylates residue Ser366 of STING, a screen of 272 recombinant protein kinases was performed at KINEXUS (Vancouver, Canada). Briefly, peptide S366 (ELLISGMEK) or A366 (ELLIAGMEK) was mixed with individual protein kinases in the presence of [γ-^{33}P] ATP. After removing unreacted [γ-^{33}P] ATP from the reaction, radioactivity was quantified in a scintillation counter. The radioactivity of S366 was compared with that of A366.

ACCESSION NUMBERS

The Gene Expression Omnibus accession number for microarray data reported in this paper is GSE51199.

SUPPLEMENTAL INFORMATION

Supplemental Information includes Extended Experimental Procedures and six figures and can be found with this article online at http://dx.doi.org/10.1016/j.cell.2013.09.049.

AUTHOR CONTRIBUTIONS

H.K. carried out most of the experiments, and K.K. purified STING. G.N.B. wrote the manuscript.

ACKNOWLEDGMENTS

We thank Delia Gutman for technical assistance, Biju Issac for gene array analysis, and George McNamara for confocal microscopy analysis. This work was funded in part by grants R01AI079336 and UO1AI083015.

Received: August 13, 2013
Revised: September 16, 2013
Accepted: September 25, 2013
Published: October 10, 2013

REFERENCES

Abe, T., Harashima, A., Xia, T., Konno, H., Konno, K., Morales, A., Ahn, J., Gutman, D., and Barber, G.N. (2013). STING recognition of cytoplasmic DNA instigates cellular defense. Mol. Cell *50*, 5–15.

Ablasser, A., Goldeck, M., Cavlar, T., Deimling, T., Witte, G., Röhl, I., Hopfner, K.P., Ludwig, J., and Hornung, V. (2013). cGAS produces a 2′-5′-linked cyclic dinucleotide second messenger that activates STING. Nature *498*, 380–384.

Ahn, J., Gutman, D., Saijo, S., and Barber, G.N. (2012). STING manifests self DNA-dependent inflammatory disease. Proc. Natl. Acad. Sci. USA *109*, 19386–19391.

Alers, S., Löffler, A.S., Wesselborg, S., and Stork, B. (2012). Role of AMPK-mTOR-Ulk1/2 in the regulation of autophagy: cross talk, shortcuts, and feedbacks. Mol. Cell. Biol. *32*, 2–11.

Alexander, A., and Walker, C.L. (2011). The role of LKB1 and AMPK in cellular responses to stress and damage. FEBS Lett. *585*, 952–957.

Blasius, A.L., and Beutler, B. (2010). Intracellular toll-like receptors. Immunity *32*, 305–315.

Burdette, D.L., Monroe, K.M., Sotelo-Troha, K., Iwig, J.S., Eckert, B., Hyodo, M., Hayakawa, Y., and Vance, R.E. (2011). STING is a direct innate immune sensor of cyclic di-GMP. Nature *478*, 515–518.

Civril, F., Deimling, T., de Oliveira Mann, C.C., Ablasser, A., Moldt, M., Witte, G., Hornung, V., and Hopfner, K.P. (2013). Structural mechanism of cytosolic DNA sensing by cGAS. Nature *498*, 332–337.

Diner, E.J., Burdette, D.L., Wilson, S.C., Monroe, K.M., Kellenberger, C.A., Hyodo, M., Hayakawa, Y., Hammond, M.C., and Vance, R.E. (2013). The innate immune DNA sensor cGAS produces a noncanonical cyclic dinucleotide that activates human STING. Cell Rep. *3*, 1355–1361.

Fu, D., Wakabayashi, Y., Lippincott-Schwartz, J., and Arias, I.M. (2011). Bile acid stimulates hepatocyte polarization through a cAMP-Epac-MEK-LKB1-AMPK pathway. Proc. Natl. Acad. Sci. USA *108*, 1403–1408.

Gall, A., Treuting, P., Elkon, K.B., Loo, Y.M., Gale, M., Jr., Barber, G.N., and Stetson, D.B. (2012). Autoimmunity initiates in nonhematopoietic cells and progresses via lymphocytes in an interferon-dependent autoimmune disease. Immunity *36*, 120–131.

Gao, P., Ascano, M., Wu, Y., Barchet, W., Gaffney, B.L., Zillinger, T., Serganov, A.A., Liu, Y., Jones, R.A., Hartmann, G., et al. (2013). Cyclic [G(2′,5′)pA(3′,5′)p] is the metazoan second messenger produced by DNA-activated cyclic GMP-AMP synthase. Cell *153*, 1094–1107.

Hardie, D.G., Ross, F.A., and Hawley, S.A. (2012). AMP-activated protein kinase: a target for drugs both ancient and modern. Chem. Biol. *19*, 1222–1236.

Henault, J., Martinez, J., Riggs, J.M., Tian, J., Mehta, P., Clarke, L., Sasai, M., Latz, E., Brinkmann, M.M., Iwasaki, A., et al. (2012). Noncanonical autophagy is required for type I interferon secretion in response to DNA-immune complexes. Immunity *37*, 986–997.

Ishikawa, H., and Barber, G.N. (2008). STING is an endoplasmic reticulum adaptor that facilitates innate immune signalling. Nature *455*, 674–678.

Ishikawa, H., Ma, Z., and Barber, G.N. (2009). STING regulates intracellular DNA-mediated, type I interferon-dependent innate immunity. Nature *461*, 788–792.

Jin, L., Waterman, P.M., Jonscher, K.R., Short, C.M., Reisdorph, N.A., and Cambier, J.C. (2008). MPYS, a novel membrane tetraspanner, is associated with major histocompatibility complex class II and mediates transduction of apoptotic signals. Mol. Cell. Biol. *28*, 5014–5026.

Kawai, T., and Akira, S. (2011). Toll-like receptors and their crosstalk with other innate receptors in infection and immunity. Immunity *34*, 637–650.

Kranzusch, P.J., Lee, A.S., Berger, J.M., and Doudna, J.A. (2013). Structure of human cGAS reveals a conserved family of second-messenger enzymes in innate immunity. Cell Rep. *3*, 1362–1368.

Mizushima, N. (2010). The role of the Atg1/ULK1 complex in autophagy regulation. Curr. Opin. Cell Biol. *22*, 132–139.

Saitoh, T., Fujita, N., Hayashi, T., Takahara, K., Satoh, T., Lee, H., Matsunaga, K., Kageyama, S., Omori, H., Noda, T., et al. (2009). Atg9a controls dsDNA-driven dynamic translocation of STING and the innate immune response. Proc. Natl. Acad. Sci. USA *106*, 20842–20846.

Sun, W., Li, Y., Chen, L., Chen, H., You, F., Zhou, X., Zhou, Y., Zhai, Z., Chen, D., and Jiang, Z. (2009). ERIS, an endoplasmic reticulum IFN stimulator, activates innate immune signaling through dimerization. Proc. Natl. Acad. Sci. USA *106*, 8653–8658.

Sun, L., Wu, J., Du, F., Chen, X., and Chen, Z.J. (2013). Cyclic GMP-AMP synthase is a cytosolic DNA sensor that activates the type I interferon pathway. Science *339*, 786–791.

Tamura, T., Yanai, H., Savitsky, D., and Taniguchi, T. (2008). The IRF family transcription factors in immunity and oncogenesis. Annu. Rev. Immunol. *26*, 535–584.

Tanaka, Y., and Chen, Z.J. (2012). STING specifies IRF3 phosphorylation by TBK1 in the cytosolic DNA signaling pathway. Sci. Signal. *5*, ra20.

Tooze, S.A., Jefferies, H.B., Kalie, E., Longatti, A., McAlpine, F.E., McKnight, N.C., Orsi, A., Polson, H.E., Razi, M., Robinson, D.J., and Webber, J.L. (2010). Trafficking and signaling in mammalian autophagy. IUBMB Life *62*, 503–508.

Woodward, J.J., Iavarone, A.T., and Portnoy, D.A. (2010). c-di-AMP secreted by intracellular Listeria monocytogenes activates a host type I interferon response. Science *328*, 1703–1705.

Zhang, X., Shi, H., Wu, J., Zhang, X., Sun, L., Chen, C., and Chen, Z.J. (2013). Cyclic GMP-AMP containing mixed phosphodiester linkages is an endogenous high-affinity ligand for STING. Mol. Cell *51*, 226–235.

Zhong, B., Yang, Y., Li, S., Wang, Y.Y., Li, Y., Diao, F., Lei, C., He, X., Zhang, L., Tien, P., and Shu, H.B. (2008). The adaptor protein MITA links virus-sensing receptors to IRF3 transcription factor activation. Immunity *29*, 538–550.